

Article

Metabolic Pathways Involved in the Drought Stress Response of *Nitraria tangutorum* as Revealed by Transcriptome Analysis

Chenggong Liu ^{1,2,†}, Na Duan ^{3,4,†}, Xiaona Chen ^{3,4}, Huiqing Li ^{1,2}, Xiulian Zhao ^{1,2}, Puzeng Duo ^{3,4}, Ji Wang ⁵ and Qinghe Li ^{1,2,*} 

¹ Research Institute of Forestry, Chinese Academy of Forestry, Beijing 100091, China; liucgw1q@163.com (C.L.); lihuiqing@caf.ac.cn (H.L.); zhaoxl@caf.ac.cn (X.Z.)

² Key Laboratory of Tree Breeding and Cultivation, National Forestry and Grassland Administration, Beijing 100091, China

³ Experimental Center of Desert Forestry, Chinese Academy of Forestry, Bayan Nur 015200, China; 15149816558@163.com (N.D.); xiaonasl@126.com (X.C.); duopuzeng0065@163.com (P.D.)

⁴ Ulan Buh Desert Comprehensive Control National Permanent Scientific Research Base, National Forestry and Grassland Administration, Bayan Nur 015200, China

⁵ College of Desert Control Science and Engineering, Inner Mongolia Agricultural University, Hohhot 010010, China; wangji1957@163.com

* Correspondence: tsinghel@caf.ac.cn; Tel.: +86-010-62889658

† These authors contributed equally to this paper.

Abstract: Drought resistance in plants is controlled by multiple genes. To identify the genes that mediate drought stress responses and to assess the associated metabolic pathways in the desert shrub *Nitraria tangutorum*, we conducted a transcriptome analysis of plants under control (maximum field capacity) and drought (20% of the maximum field capacity) conditions. We analyzed differentially expressed genes (DEGs) of *N. tangutorum* and their enrichment in the KEGG metabolic pathways database, and explored the molecular biological mechanisms underlying the answer to its drought tolerance. Between the control and drought groups, 119 classified metabolic pathways annotated 3047 DEGs in the KEGG database. For drought tolerance, nitrate reductase (NR) gene expression was downregulated, indicating that NR activity was decreased to improve drought tolerance. In ammonium assimilation, drought stress inhibited glutamine formation. Protochlorophyllide reductase (1.3.1.33) expression was upregulated to promote chlorophyll *a* synthesis, whereas divinyl reductase (1.3.1.75) expression was downregulated to inhibit chlorophyll-ester *a* synthesis. The expression of the chlorophyll synthase (2.5.1.62) gene was downregulated, which affected the synthesis of chlorophyll *a* and *b*. Overall, drought stress appeared to improve the ability to convert chlorophyll *b* into chlorophyll *a*. Our data serve as a theoretical foundation for further elucidating the growth regulatory mechanism of desert xerophytes, thereby facilitating the development and cultivation of new, drought-resistant genotypes for the purpose of improving desert ecosystems.

Keywords: transcriptome analysis; drought stress; *Nitraria tangutorum*; metabolic pathways



Citation: Liu, C.; Duan, N.; Chen, X.; Li, H.; Zhao, X.; Duo, P.; Wang, J.; Li, Q. Metabolic Pathways Involved in the Drought Stress Response of *Nitraria tangutorum* as Revealed by Transcriptome Analysis. *Forests* **2022**, *13*, 509. <https://doi.org/10.3390/f13040509>

Academic Editor: Stéphane Maury

Received: 2 March 2022

Accepted: 23 March 2022

Published: 25 March 2022

Publisher's Note: MDPI stays neutral with regard to jurisdictional claims in published maps and institutional affiliations.



Copyright: © 2022 by the authors. Licensee MDPI, Basel, Switzerland. This article is an open access article distributed under the terms and conditions of the Creative Commons Attribution (CC BY) license (<https://creativecommons.org/licenses/by/4.0/>).

1. Introduction

China is one of numerous countries worldwide that face severe water resource constraints [1,2], and climate change has exacerbated water scarcity and dryland expansion [3]. For a long time, the difficulty of ensuring sustainable water resource use has increased as global greenhouse gas emissions and population density have increased, resulting in continuous temperature increases of varying magnitudes in different regions and an uneven distribution of water resources [4]; this has resulted in increased drought hazards and water shortages throughout China [5].

Perception of and adaptation to habitat change are primary challenges for the reproduction, development, and survival of all living organisms on the planet [6]. Water is one of

the most important environmental constraints on plant survival [7]. Drought restricts plant growth at all stages of growth and development and is regarded as one of the most severe environmental stressors [4,8,9], particularly in arid areas, where plants frequently experience water scarcity stress, a condition known as drought stress [10]. Additionally, drought affects respiration and photosynthesis [11,12], affecting plant physiological processes such as osmotic regulation, protein synthesis, and photosynthate transportation [13–16]. Water scarcity can eventually have a negative impact on crops' and trees' survival, growth, and productivity [17–19]. According to current research and evaluations of global climate characteristics, the limiting effect of water in desert areas is becoming increasingly difficult [20]. Thus, the mechanisms by which plants in arid and desert areas respond to water stress will undoubtedly become a focus of botanical research.

Nitraria tangutorum Bobr. (family Zygophyllaceae) is native to China [21], and is a small, unique, and typical desert sand-fixing shrub distributed in the arid and desert areas of Inner Mongolia, China [22]. As an important component of desert flora, *N. tangutorum* is resistant to multiple stresses, including wind erosion [23], sand burial [24], drought [25], salt, and alkali stresses [26,27]. Much of this resistance is related to its well-developed root system, small and fleshy leaves, and easily propagated branches. Therefore, *N. tangutorum* plays a key role in preventing wind erosion, fixing sand, optimizing the soil's physical and chemical properties, and maintaining vegetation diversity in desert areas. Furthermore, *N. tangutorum* is a significant source of economic income for the local population; for example, their fruits are known as "desert cherry" and are used to produce medicines and drinks [28], and its litter (e.g., dry branches and fallen leaves) is frequently used as firewood by residents [29]. However, structural plants in desert areas are being affected in multiple ways due to environmental damage, rising temperatures, and increasing drought intensity, in addition to their characteristic poor growth rates, decreased seed-setting rates, and increased mortality rates. These important wild resources, which are represented by *N. tangutorum*, are in danger because of drought.

As a key environmental stressor, water stress triggers diverse plant responses from the physiological and ecological levels to the molecular biology level [30,31]. Generally, when plants are threatened by external drought, they guard themselves from the deleterious stimulus of environmental fluctuations by initiating and regulating the differential expression of drought tolerance genes [32]. Drought tolerance in plants, on the other hand, is an extremely complicated process that is controlled by multiple genes at the same time [33,34]. High-throughput RNA sequencing (RNA-seq) provides a new convenient way to study the theory of plant resistance and has become a powerful tool to reveal drought stress signaling pathways and predict gene functions [31,35], and the analysis of transcriptome data could elucidate gene functions to reveal the molecular mechanisms underlying specific biological processes [36]. Currently, RNA-seq studies indicate that many drought tolerance genes are in multiple plants, e.g., poplar [37,38], soybean [39,40], and maize [32,41,42]. Unfortunately, most of the research on the drought tolerance of *N. tangutorum* in arid areas has focused on physiological and biochemical processes [43–46], while research on the molecular mechanisms underlying these physiological and biochemical processes is relatively limited; thus, the elucidation of drought-resistance mechanisms has been hindered. In this study, the objectives were to provide information on the genes and possible mechanisms regulating the growth and drought tolerance of sand xerophytes using *N. tangutorum* as a case study. The information obtained herein may be useful in the development and cultivation of new drought-resistant plant varieties.

2. Materials and Methods

2.1. Plant Materials and Experimental Design

N. tangutorum plants in the Ulan Buh desert (Inner Mongolia, China) were selected for investigation in this study. Seeds were collected from the same wild *N. tangutorum* plant that were vigorously growing in the Ulan Buh desert in August 2014 to ensure the genetic homogeneity of the experimental plants. In mid-March 2015, the seedlings were grown in

nutrient pots in the Chinese Academy of Forestry's Desert Forestry Experimental Center greenhouse (106°43' E, 40°24' N) and watered with underground water. The soil matrix was composed of local farmland topsoil and low-salinity, fine sand, which were screened and mixed in equal amounts (1:1, *v/v*). In early May 2015, seedlings of relatively uniform sizes were transplanted into our independently developed PVC material barrels (40 cm height × 16 cm in diameter), one plant per barrel; then, they were randomly assigned to the drought treatment (T) and control (CK) groups. The groups were comprised of 6 replicates with 60 plants per replicate. The soil moisture content was maintained at 100% of the field capacity (FC) (i.e., 20.3%) in the CK group, and at 20–40% of the FC in the T group. When the treated soil water content was below the experimental level, moderate watering was carried out with a syringe until it met the experimental level. Meanwhile, the soil water content was determined by the gravimetric method, weighing once every morning at 9 o'clock for 60 days. Plant survival was guaranteed in both treatment groups, and other routine maintenance and management measures for seedlings reflected standard field management practices.

2.2. Complementary DNA Library Construction and RNA Sequencing

The RNAsimple Total RNA Kit (TIANGEN, Beijing, China) was used to isolate the total RNA from leaf tissue samples of *N. tangutorum* (mixed sampling was conducted after 60 days of drought treatment; each treatment used three biological replicates, and samples were quickly put into a −80 °C refrigerator for later use). A total amount of 1.5 µg RNA per sample was used as input material for the RNA sample preparations. Sequencing libraries were generated using NEBNext® Ultra™ RNA Library Prep Kit for Illumina® (NEB, Ipswich, MA, USA) following the manufacturer's recommendations. Briefly, mRNA was purified from the total RNA using poly-Toligo-attached magnetic beads. Fragmentation was carried out using divalent cations under an elevated temperature in a NEBNext First Strand Synthesis Reaction Buffer (5X). First-strand cDNA was synthesized using a random hexamer primer and M-MuLV Reverse Transcriptase (RNase H[−]). Second-strand cDNA synthesis was subsequently performed using DNA Polymerase I and RNase H. The remaining overhangs were converted into blunt ends via exonuclease/polymerase activities. After adenylation of the 3' ends of the DNA fragments, a NEBNext Adaptor with a hairpin loop structure were ligated to prepare for hybridization. In order to select cDNA fragments of the preferable length of 250~300 bp, the library fragments were purified with AMPure XP system (Beckman Coulter, Beverly, CA, USA). Then 3 µL USER Enzyme (NEB, Ipswich, MA, USA) was used with size-selected, adaptor-ligated cDNA at 37 °C for 15 min, followed by 5 min at 95 °C before PCR analysis. Then, PCR analysis was performed with Phusion High-Fidelity DNA polymerase, Universal PCR primers, and an Index (X) Primer. At last, the PCR products were purified (AMPure XP system), and the library quality was assessed on the Agilent Bioanalyzer 2100 system. All the above work, including the construction of the cDNA library and RNA-seq, were completed at Novogene Technology Co., Ltd. (Beijing, China).

2.3. Enrichment Analysis of Differentially Expressed Genes

DESeq software [47] was used to analyze and screen the differentially expressed genes (DEGs). The numbers of DEGs between the CK and T groups were statistically analyzed, including upregulated genes and downregulated genes. The screening thresholds for the DEGs in the CK group were $\text{padj} < 0.05$ and $|\log_2(\text{FoldChange})| > 1$.

GOseq software was used to annotate all the DEGs into the gene ontology (GO) database, calculate the number of genes annotated to each GO term (biological process, molecular function, and cell composition), analyze significantly enriched GO terms of *N. tangutorum* compared with the whole-genome background, and determine the biological function of the DEGs. Screening was done by setting a cutoff point of less than or equal to 0.05. GO terms that met this standard were considered to be "significantly rich".

All the DEG sequences were annotated to the Kyoto Encyclopedia of Genes and Genomes (KEGG) database using KOBAS 2.0 software [48], and the signal transduction pathways and major biochemical metabolic pathways involved in the identified DEGs were then determined. A p -value threshold of ≤ 0.05 was set for significant enrichment.

2.4. Verification of RNA-Seq Data by Quantitative Real-Time PCR

Ten DEGs of *N. tangutorum* were randomly selected, and the differences in their expression levels were verified by quantitative real-time PCR (qRT-PCR). Ten primers were designed (Table 1). Then, 1.0 μ g total RNA of each sample of *N. tangutorum* was reverse-transcribed with a GoldenstarTM RT6 cDNA Synthesis Kit (TSINGKE BIOTECH, Beijing, China); then, cDNA was amplified using $2 \times$ T5 Fast qPCR Mix (SYBR Green I) from the same company. Afterward, the relative transcript abundance of gene expression level was analyzed by a $2^{-\Delta\Delta C_t}$ method for each sample.

Table 1. Information about of ten primers.

Gene ID	Forward Primer (5'–3')	Reverse Primer (5'–3')
Cluster-40906.35332	TTCCTCCCCACGCACTTTTC	CCAGTTCGGCCTGTCATTC
Cluster-40906.11509	AACTCTGAGCAGTAACCAAGCAA	ACTCTGAATTAGAATATGCAACCGA
Cluster-40906.56890	ATCCAAGCGACATGGCGAA	TTCTGCAGGAAACTTGAAGTCGTAG
Cluster-40906.174397	CCAATGATACCGCATCCAAT	ATGATCTCGGAAAAGGTGGAC
Cluster-28726.1	CCATCATCACACAGAATGTAAAA	TCCAGATCGGAGTACAAAATTAC
Cluster-40906.57689	TTGCTACCCCAAACCTGACTTC	CATTTCTCTTCCGCCTCAC
Cluster-40906.102382	ATTCAACCCAATTCTCACTTTCTT	ATAACGCAGGAGACGCACCA
Cluster-40906.114615	ACATCCTTCTTTCCATCCTCCA	GAATGATGTATGACCGACCACC
Cluster-40906.35748	TCCGGGAAATTGAGAGTTGC	AAGGGGGTGAGGATGAGAAA
Cluster-40906.176764	AGAAGCTGGGGAAAATGGGTAT	GAGTTGGGGGAAGTTGAGGAC
NsActin	GGAATCCACGAGACCACCTACA	GATTGATCCTCCGATCCAGACA

3. Results

3.1. RNA-Seq Analysis and Transcript Splicing

The data results showed that the RNA-seq of *N. tangutorum* yielded 48,422,264 (CK-2) to 64,926,978 (T-3) raw reads per experimental group. The clean reads in each group accounted for 98.16% (CK-1), 97.54% (CK-2), 98.22% (CK-3), 98.31% (T-1), 98.72% (T-2), and 98.15% (T-3) of the raw reads, respectively; these high proportions guaranteed the splicing of transcripts. The GC content in each treatment group ranged from 45.62% to 46.24%, and the error rate was only 0.03% (see Supplementary Data in Table S1).

The Corset hierarchical clustering results showed that the transcript sequences were combined into 332,420 transcripts and 276,423 unigenes (see Supplementary Data in Table S2). The transcripts ranged in length from 201 to 26,379 nucleotides, with a mean length of 966 nucleotides. The minimum transcript length needed to cover 50% of the genome (N50) was 1554 nucleotides. The unigene length ranged from 201 to 26,379 nucleotides, with a mean length of 1107 nucleotides; the N50 was 1628 nucleotides.

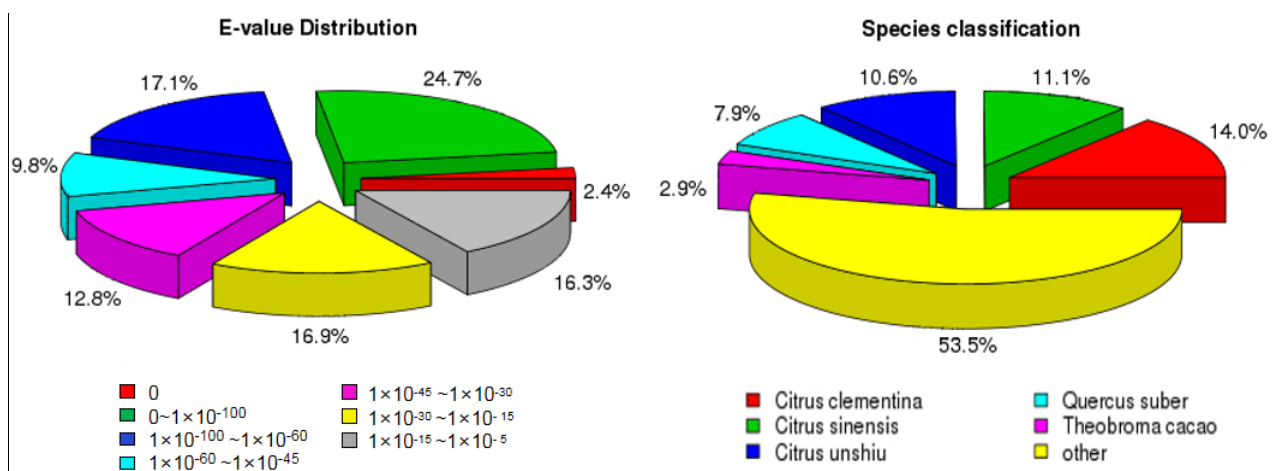
3.2. Gene Function Annotation

Through database comparison and analysis, 32,048 unigenes of *N. tangutorum* were annotated in the seven databases (Table 2). The comparison results indicated that 25,380 unigenes were successfully annotated, accounting for 9.18% of the total unigenes; 195,214 unigenes were successfully annotated by at least one of the databases, accounting for 70.62%; and 29.38% of unigenes failed, possibly indicating the presence of novel genes.

Table 2. Unigenes of *N. tangutorum* were compared with seven databases.

Database Name	Unigene Numbers	Ratio (%)
Nr (NCBI, Non-redundant Protein Sequences Database)	176,393	63.81
Nt (NCBI, Nucleotide Sequences Database)	116,688	42.21
KO (KEGG Orthology)	70,817	25.61
Swiss-Prot (Annotated Protein Sequence Database)	129,949	47.01
PFAM (Family Protein Database)	122,945	44.47
GO (Gene Ontology Database)	122,945	44.47
KOG (euKaryotic Ortholog Groups)	48,287	17.46
All databases	25,380	9.18
At least one database	195,214	70.62
Total unigenes	276,423	100

The E-values and species distributions for the 176,393 genes functionally annotated in the Nr database (Figure 1) showed the largest distribution of unigenes at $0-1 \times 10^{-100}$, accounting for 27.4% of the total. According to the annotation results of species distribution, the annotated proportion of all unigenes in citrus, sweet orange, kumquat, *Quercus* sp., and cacao accounted for 14.0%, 11.1%, 10.6%, 7.9%, and 2.9% of the total gene number, respectively.

**Figure 1.** Distribution of unigenes: **Left**, E-value distribution map of Nr in the NCBI database; **right**, species distribution map of Nr.

3.3. KEGG Functional Classification

Figure 2 shows that 70,817 genes were enriched in 19 metabolic pathways. Among the enriched genes, 1703 were involved in signal transduction in the physiological and metabolic processes of *N. tangutorum*, and 2174 were related to environmental adaptation.

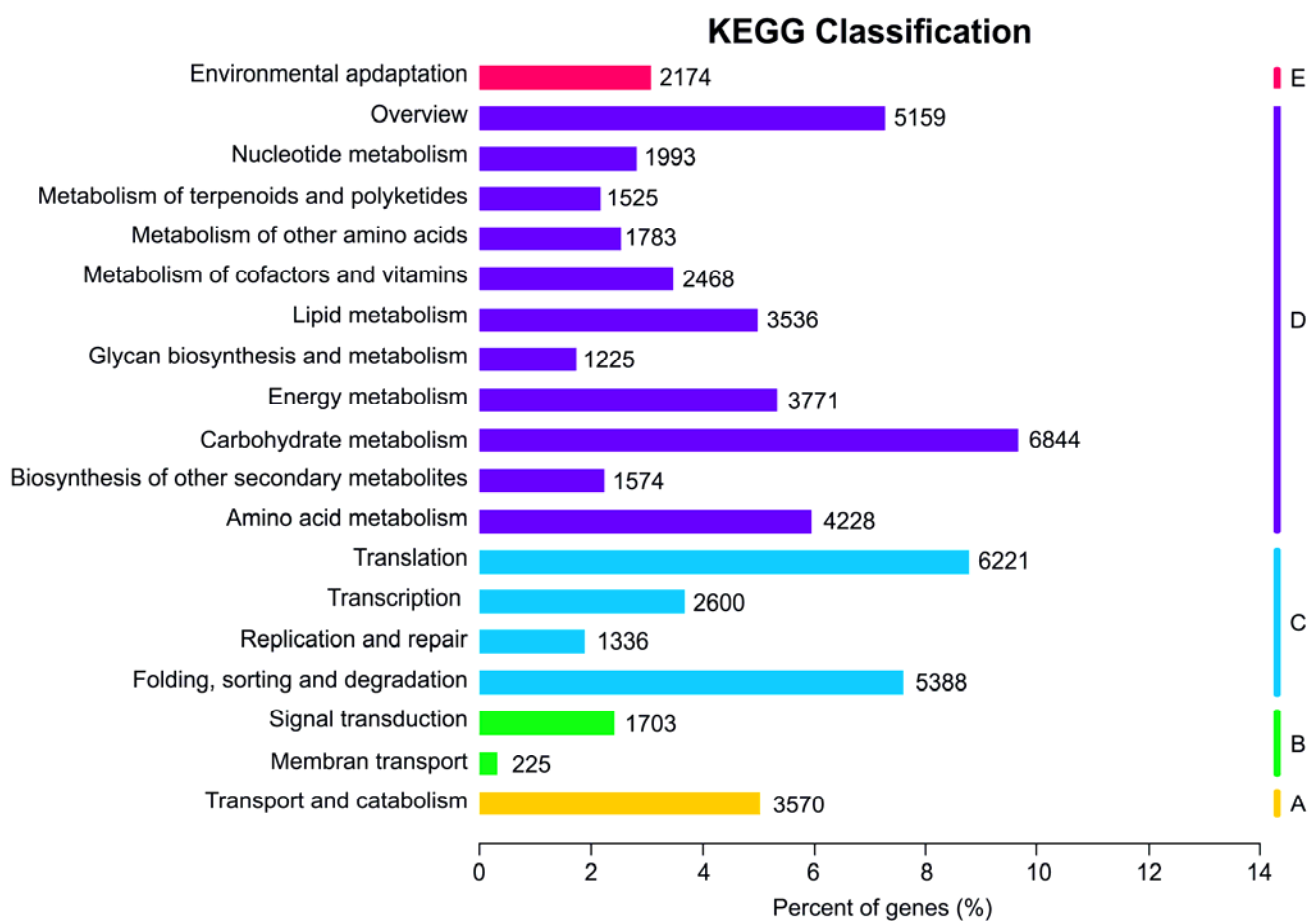


Figure 2. KEGG functional classifications.

3.4. DEGs Analysis

Transcriptome data were analyzed to study the regulatory mechanism of *N. tangutorum* under drought stress. The DEGs in each treatment group were used to create a volcano map to reflect the gene expression (Figure 3). There were 10,229 DEGs between the T and CK treatments, including 4767 upregulated and 5462 downregulated genes. The DEGs indicated that, when *N. tangutorum* was subjected to drought stress, the molecular mechanisms of the drought tolerance genes were activated. In addition, the expression of some genes was upregulated while that of other genes was inhibited. The significant difference analysis of gene function between the T group and the CK group showed that 16 and 14 genes were upregulated and downregulated among the top 30 genes with significant differentially expressed genes, respectively (Table 3). These genes mainly code for heme, peroxidase, hydrolase, redox enzymes, dehydrogenases, peptidases, hydrogen phosphate salt synthases, and transposase, which are related to plant stress reactions, signal transduction, amino acid metabolism, and oxidation or reduction.

Table 3. Top 30 genes showing significant differential expression under drought stress.

Gene ID	log ₂ Fold Change	p-Value	Description
Cluster-40906.113941	−3.5898	7.38×10^{-74}	Oxidoreductase activity//chlorophyllide <i>a</i> oxygenase (overall) activity//2 iron, 2 sulfur cluster binding
Cluster-40906.41614	4.6013	1.57×10^{-72}	Unfolded protein binding//ATP binding
Cluster-40906.93310	−2.0399	1.15×10^{-67}	Protein binding
Cluster-40906.110044	−5.814	1.43×10^{-66}	Calcium ion binding
Cluster-40906.175859	4.7681	1.49×10^{-60}	DNA binding//transposase activity//ATP binding//unfolded protein binding
Cluster-40906.104561	−4.0125	1.19×10^{-53}	Transporter activity
Cluster-40906.116353	−2.4038	1.41×10^{-53}	Chitinase activity
Cluster-40906.83443	4.8401	9.86×10^{-53}	Unfolded protein binding//ATP binding
Cluster-40906.62892	3.2606	7.27×10^{-52}	Hypothetical protein CUMW_183970
Cluster-40906.109750	−7.2303	1.29×10^{-51}	−
Cluster-40906.123767	1.5802	2.95×10^{-50}	DnaJ homolog subfamily B member 7 isoform X2
Cluster-40906.107883	2.056	7.53×10^{-50}	Chlorophyll <i>a-b</i> -binding protein CP26, chloroplastic-like
Cluster-40906.175857	5.4749	2.58×10^{-48}	Heat shock protein 90-1
Cluster-40906.108887	−2.4863	3.24×10^{-48}	Transmembrane transport
Cluster-40906.121414	−4.0105	2.51×10^{-46}	Phosphatidylinositol-4-phosphate binding
Cluster-40906.112950	−14.664	1.01×10^{-45}	Zinc ion binding
Cluster-40906.115294	5.5761	1.08×10^{-45}	Heme binding//peroxidase activity
Cluster-40906.112156	10.614	2.10×10^{-43}	Hydrolase activity, hydrolyzing O-glycosyl compounds
Cluster-40906.147611	3.1736	1.04×10^{-42}	Catalytic activity//oxidoreductase activity//3-hydroxyacyl-CoA dehydrogenase activity//peptidase activity//hydrolyase activity
Cluster-40906.119123	1.4464	4.56×10^{-42}	Protein binding
Cluster-40906.111055	−1.3917	2.64×10^{-41}	ATP binding//GTP binding//GTPase activity//cytidylate kinase activity//ATPase activity
Cluster-40906.117956	−7.1941	3.62×10^{-41}	Adenyl-nucleotide exchange factor activity//transcription factor activity, sequence-specific DNA binding//exodeoxyribonuclease VII activity//protein homodimerization activity//unfolded protein binding//chaperone binding//protein binding, bridging//protein tag//motor activity//structural molecule activity//acid-amino acid ligase activity//receptor binding
Cluster-40906.105679	3.2201	1.26×10^{-40}	4-Hydroxy-3-methylbut-2-en-1-yl diphosphate synthase activity
Cluster-40906.35332	3.1073	2.86×10^{-39}	Protein binding//catalytic activity
Cluster-40906.111273	−1.6128	7.15×10^{-38}	Transcription factor activity, sequence-specific DNA binding
Cluster-40906.111303	4.1859	1.28×10^{-37}	Hypothetical protein B456_006G088300
Cluster-40906.118097	2.0982	4.43×10^{-37}	−
Cluster-40906.89392	3.4364	1.82×10^{-36}	Protein dimerization activity
Cluster-40906.129546	−4.631	3.31×10^{-36}	Alcohol dehydrogenase 1
Cluster-40906.49184	−5.5647	4.42×10^{-36}	Structural constituent of ribosome

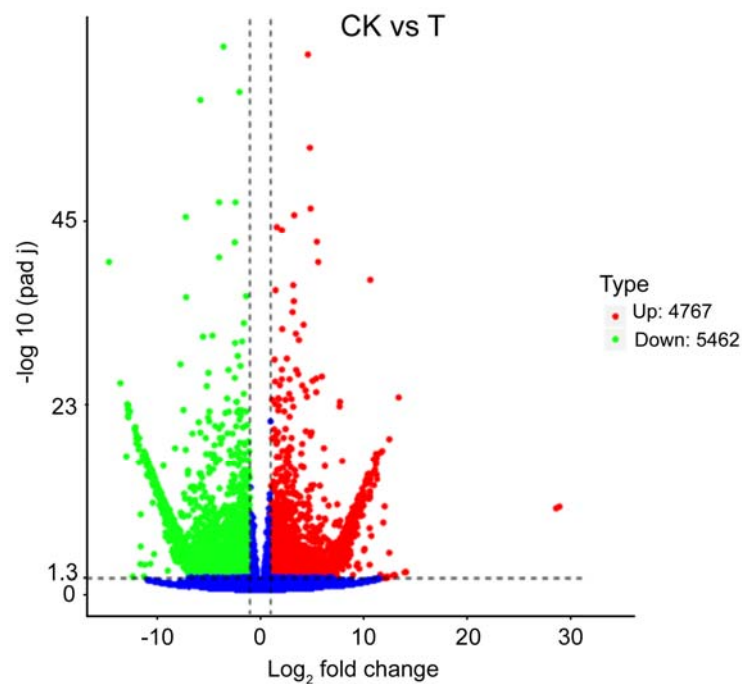


Figure 3. Volcano map of DEGs in the treatment groups.

3.5. KEGG Enrichment Analysis

In order to identify the main signal transduction and biological metabolic pathways of *N. tangutorum* in response to drought stress, the KEGG pathway analysis of DEGs under drought stress was conducted in this study. In the KEGG database, 3047 DEGs of 119 classified metabolic pathways were annotated, among which 14 pathways showed significant enrichment (p -value less than 0.05). As shown in Table 4, these pathways were mainly related to the functions of ribosomes (177 members, 21.5%), and were followed by protein processing in the endoplasmic reticulum (139 members, 16.9%), spliceosomes (110 members, 13.4%), plant hormone signal transduction (101 members, 12.3%), and starch and sucrose metabolism (98 members, 11.9%). The other nine metabolic pathways involved 198 members, accounting for 24.1% of the total.

Table 4. Significant enrichment of metabolic pathways in the KEGG database in the drought stress vs. control groups comparison.

KEGG Pathway	ID	DEG Number	p -Value
Ribosome	ko03010	177	1.26×10^{-7}
Plant hormone signal transduction	ko04075	101	1.86×10^{-6}
Protein processing in endoplasmic reticulum	ko04141	139	1.69×10^{-5}
Porphyrin and chlorophyll metabolism	ko00860	44	0.001141408
Spliceosome	ko03040	110	0.001860469
Phenylalanine, tyrosine, and tryptophan biosynthesis	ko00400	34	0.005868948
Starch and sucrose metabolism	ko00500	98	0.006867847
Anthocyanin biosynthesis	ko00942	8	0.011943248
Flavonoid biosynthesis	ko00941	17	0.013126286
Alpha-linolenic acid metabolism	ko00592	29	0.032232635
Taurine and hypotaurine metabolism	ko00430	12	0.034211087
Photosynthesis (antenna proteins)	ko00196	26	0.035911307
Limonene and pinene degradation	ko00903	14	0.038622556
Stilbenoid, diarylheptanoid, and gingerol biosynthesis	ko00945	14	0.046974746

The number of upregulated DEGs in the endoplasmic reticulum protein-processing process was 104, which was the largest among all upregulated DEGs, followed by 67 upregulated

DEGs in the metabolism of starch and sucrose; 59 in spliceosome; 40 in the signal transduction of plant hormones; and 37 in the carbon sequestration in photosynthetic organisms (Figure 4). The range of q-values was [0, 1]. The closer the q-value is to zero, the more significant the enrichment is. The DEGs involved in starch and sucrose metabolism, spliceosome, endoplasmic reticulum protein processing, porphyrin and chlorophyll metabolism, photosynthesis (antenna protein), and flavonoid biosynthesis were all significantly enriched. These data indicate that *N. tangutorum* can resist water deficiency by modulating and sensitizing the function of the genes involved in these biosynthetic and metabolic pathways.

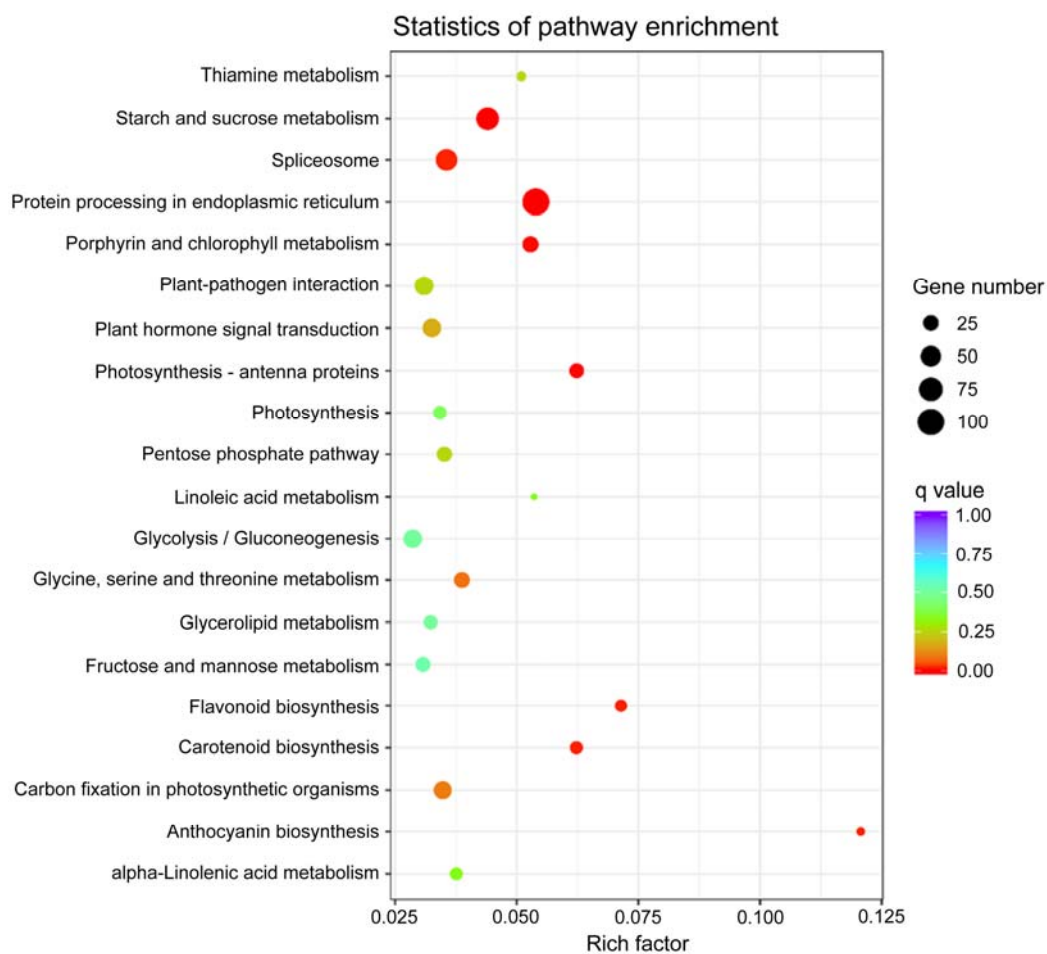


Figure 4. KEGG pathway enrichment analysis of upregulated DEGs in *N. tangutorum*. The horizontal axis represents the enrichment factor corresponding to each pathway. The vertical axis represents the pathway name. Dot colors denote the magnitude of q-values, and their sizes denote the number of DEGs.

3.6. Nitrogen Metabolism

In the nitrogen metabolism pathway under drought stress (Figure 5), nitrate reductase (*NR*; 1.7.1.4 1.7.7.1, 1.7.1.15, 1.7.2.2) is a rate-limiting enzyme, and its activity directly affects the nitrogen utilization efficiency of plants. As shown in the figure, during the reduction of nitrate to nitrite, the expression of the *NR* gene was downregulated. However, during nitrite formation in the process of ammonia assimilation, *NiR* gene expression was not changed, whereas the expression of the glutamine synthetase (*GS*; 6.3.1.2) gene was downregulated. In the glutamate synthetase (*GOGAT*) pathway, which catalyzes the formation of glutamate, *NADH-GOGAT* (1.4.1.13 and 1.4.1.14) expression was downregulated, while *Fd-GOGAT* (1.4.7.1) expression was upregulated or downregulated. In the formamide synthesis pathway, the expression of the formamide enzyme (3.5.1.49) gene was down-

regulated. During the conversion of carbon dioxide to bicarbonate, the expression of the carbonic anhydrase gene was either upregulated or downregulated.

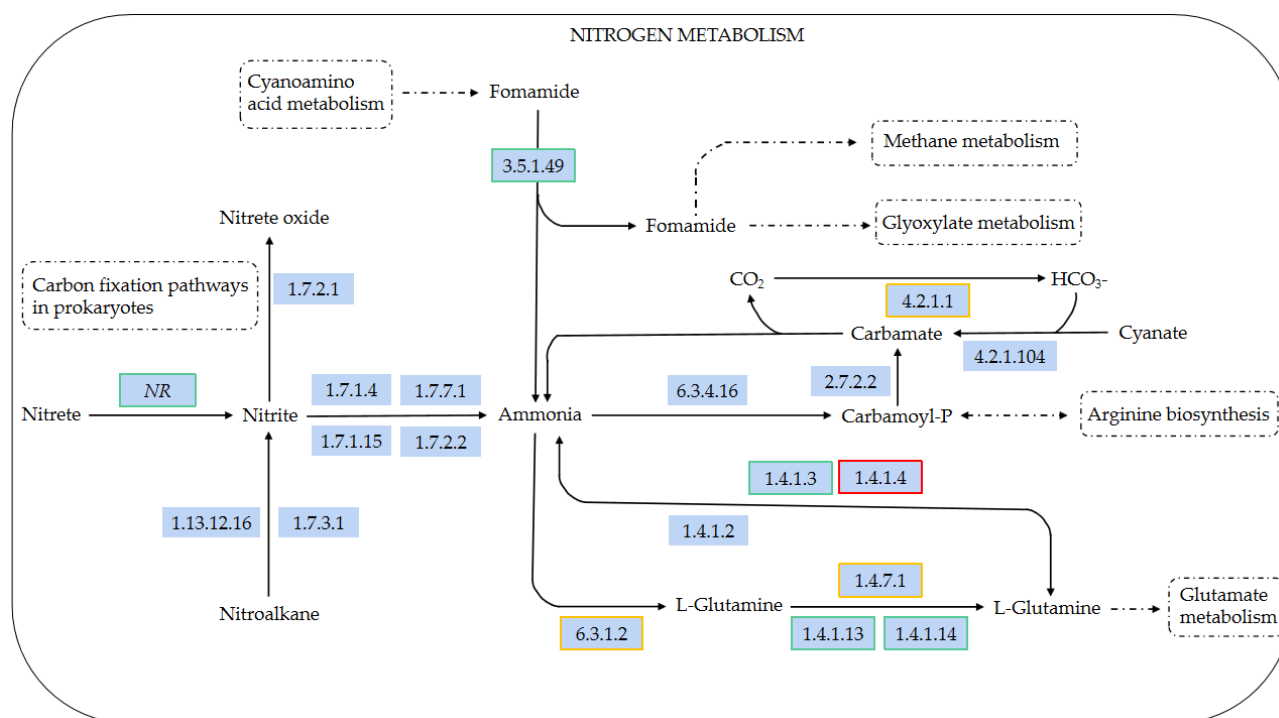


Figure 5. Nitrogen metabolism pathway of *N. tangutorum* under drought stress: (1) Red boxes denote the upregulated genes; green boxes denote the downregulated genes; yellow boxes denote the up/downregulated genes. (2) Black solid arrows denote molecular interactions or relationships; dotted arrows denote indirect effects; dotted boxes denote other signal pathway maps. (3) Letters and numbers on a blue background denote genes or enzymes involved in metabolic pathways. NR: nitrate reductase (NAD(P)H); 1.7.2.1: nitrite reductase (NO-forming); 1.13.12.16: nitronate monooxygenase; 1.7.3.1: nitroalkane oxidase; 1.7.1.4: nitrite reductase (NAD(P)H); 1.7.7.1: ferredoxin-nitrite reductase; 1.7.1.15: nitrite reductase (NADH) large subunit; 1.7.2.2: nitrite reductase (cytochrome c-552); 3.5.1.49: formamidase; 1.4.1.2: glutamate dehydrogenase; 1.4.1.3: glutamate dehydrogenase (NAD(P)+); 1.4.1.4: glutamate dehydrogenase (NADP+); 6.3.1.2: glutamine synthetase; 6.3.4.16: carbamoyl-phosphate synthase (ammonia); 1.4.1.13: glutamate synthase (NADH); 1.4.1.14: glutamate synthase (NADH); 1.4.7.1: glutamate synthase (ferredoxin); 2.7.2.2: carbamate kinase; 4.2.1.104: cyanate lyase; 4.2.1.1: carbonic anhydrase.

3.7. Metabolism of Porphyrin and Chlorophyll

Table 5 shows that in the alpha-linolenic acid (ALA) synthesis pathway, the expression of the tRNA synthase gene was downregulated, while the expression of the glutamine tRNA reductase gene was upregulated, and that of the glutamine-1-hemialdehyde transaminase gene was mainly downregulated. The expression of the bile pigment synthase, uroporphyrin procarboxylase, and protoporphyrinogen oxidase genes and the ferrous heme synthase and *COX15* genes was upregulated. The expression of the ferrochelatase gene and the magnesium chelatase H subunit gene was upregulated and downregulated. We also found from Table 5 that the expression of the prochlorophyll reductase, chlorophyll *b* reductase, and 7-hydroxychlorophyll *a* reductase genes was upregulated, but the diethylene reductase genes' expression was downregulated. In addition, during the transformation of chlorophyll *a* into chlorophyllin *a*, and chlorophyll *b* into chlorophyllin *b*, the expression of the chlorophyll enzyme and *CHIP* genes was downregulated. The expression of the *PAO* gene was upregulated in magnesium removal and transplant-based reactions.

Table 5. Effect of drought treatment on relating functional genes of porphyrin and chlorophyll metabolism in *N. tangutorum*.

Enzyme	Gene Name	Gene ID	Up/Downregulated
6.1.1.17	Glutamine tRNA synthetase	Cluster-40906.71722	Down
		Cluster-40906.54653	Down
1.2.1.70	Glutamyl-tNRA reductase	Cluster-40906.114395	Up
		Cluster-40906.129403	Up
5.4.3.8	Glutamate-1-hemialdehyde transaminase	Cluster-40906.192599	Up
		Cluster-40906.119289	Down
4.2.1.24	Bile pigment synthase	Cluster-40906.85742	Up
		Cluster-40906.85733	Up
		Cluster-40906.85731	Up
4.2.1.75	Uroporphyrinogen decarboxylase	Cluster-40906.104102	Up
1.3.3.4/1.3.3.15	Protoporphyrinogen oxidase	Cluster-40906.34049	Up
4.99.1.1/4.99.1.9	Ferrochelatase	Cluster-40906.121603	Up
		Cluster-40906.121607	Up
		Cluster-40906.121031	Up
		Cluster-40906.100839	Down
		Cluster-40906.93744	Down
		Cluster-40906.100841	Down
		Cluster-40906.118608	Up
2.5.1.-	Heme O ferric synthetase	Cluster-40906.59147	Up
	COX15	Cluster-40906.117245	Up
6.6.1.1	Magnesium chelatase H subgroup	Cluster-40906.137917	Up
		Cluster-40906.157365	Up
		Cluster-40906.106867	Up
		Cluster-40906.93092	Up
		Cluster-40906.118198	Up
		Cluster-40906.118566	Up
		Cluster-40906.110295	Up
		Cluster-40906.121612	Down
		Cluster-40906.103817	Down
		Cluster-40906.106857	Down
1.3.1.75	Divinyl reductase	Cluster-40906.109654	Down
1.3.1.33	Prochlorophyll reductase	Cluster-40906.168882	Up
		Cluster-40906.99070	
2.5.1.62	Chlorophyll synthase	Cluster-40906.89493	Down
1.1.1.294	Chlorophyll <i>b</i> reductase	Cluster-40906.133380	Up
		Cluster-40906.59982	Up
		Cluster-40906.59985	Down
		Cluster-40906.27543	Down
1.17.7.2	7-Hydroxymethyl chlorophyll <i>a</i> reductase	Cluster-40906.185694	Up
3.1.1.14	Chlorophyllase	Cluster-40906.151688	Down
1.14.1517	PAO	Cluster-40906.92868	Up
2.5.1.133	Chlorophyll synthase	Cluster-40906.89493	Down
1.3.1.111	CHIP	Cluster-40906.113828	Up
		Cluster-40906.113825	Down
		Cluster-40906.113826	Down

3.8. Transcriptome Data Validation

To validate the exactitude of the RNA-seq data, 10 DEGs of *N. tangutorum* were randomly selected for qRT-PCR analysis. As shown in Figure 6, the qRT-PCR test results were similar to the RNA-seq data except for two genes (Cluster-40906.102382 and Cluster-40906.114615), and the expression trends of most genes were coincident, thus verifying the reliability of the RNA-seq test results.

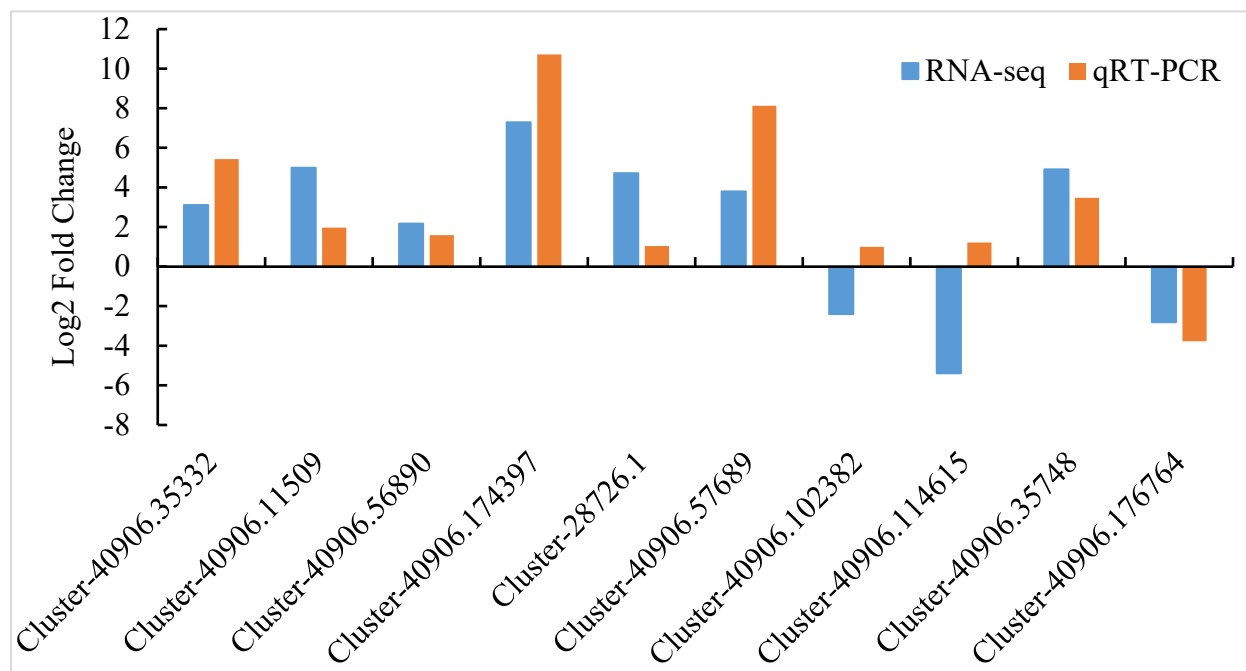


Figure 6. Comparison of qRT-PCR and RNA-seq results of 10 candidate genes in *N. tangutorum*.

4. Discussion

As *N. tangutorum* is one of the primary species in the Ulan Buh desert, explorations of its molecular responses to the arid environment in the context of a complex desert climate have significant merit. We discovered that nearly 71% of the concatenated unigene sequences were successfully annotated in the multiple databases. On querying the concatenated unigene sequences to multiple databases (Nr, Nt, KO, KOG, Swiss-Prot, GO, and PFAM). The inability to annotate the remaining sequences could be due to the following factors: (1) some ultrashort sequences were not amenable to homology comparisons [49]; (2) a temporary lack of annotation information, resulting in the corresponding functions being unannotated [50]; (3) some gene sequences lacked conserved regions, or some genes themselves were non-coding or incomplete sequences [51]. However, the proportion of unannotated genes for *N. tangutorum* was lower than in other desert plants, such as *Haloxylon ammodendron* (41%) [52], *Ammopiptanthus mongolicus* (62%) [53], *Caragana microphylla* (39%) [54], and *Hippophae rhamnoides* (43%) [55]. As a result, we thought that this result was due to *N. tangutorum* possessing unique genetic resources that distinguish it from other species.

In general, many plants enable a variety of metabolic and physiological mechanisms to ensure normal life function and protect against the damage caused by drought crises, including the activation of protein kinases, antioxidants, carotenoid, flavonoid biosynthesis, and plant hormones (e.g., ABA, JA, IAA, etc.) [32,56–58]. The KEGG pathway enrichment analysis laid the groundwork for identifying and screening active biological metabolic pathways in plants, elucidating the metabolic mechanisms activated in response to drought. The KEGG enrichment analysis revealed that the genes regulating plant hormone synthesis and signaling transduction are regulated and controlled differently under different drought conditions, and may also play a critical role in the environmental adaptation of plants (e.g., *Rosa chinensis*) [59]. In the present study, the KEGG analysis revealed that, under drought stress, the porphyrin and chlorophyll metabolism pathways of *N. tangutorum* leaves were significantly enriched. Thus, we hypothesized that the enzymes involved in chlorophyll metabolism are critical for *N. tangutorum* growth and development under drought stress. Additionally, the ribosomes, anthocyanin synthesis, flavonoid biosynthesis, plant hormone signal transduction, and other physiological reactions were also enriched, implying that

the genes encoding these pathways were a critical molecular biological pathway for *N. tangutorum* to cope with drought stress.

Plant nitrogen metabolism is primarily based on the reduction of NO_3^- to NO_2^- by NR; ammonia is generated by nitrite reductase (NiR) [60,61] and assimilated into organic nitrogen stored in plants via the GS/GOGAT cycle [62,63]. NR is a rate-limiting enzyme in nitrogen metabolism [64,65], directly regulating the reduction to NO_3^- [66,67], and affects the efficiency of plant nitrogen utilization [68]. Additionally, multiple studies have demonstrated that, when plants are severely stressed by drought, the NR gene is significantly downregulated, and NR activity is significantly reduced in plants such as *Triticum aestivum* [69], *Oryza sativa* [67], and *Hordeum vulgare* [70]. The reduction of NO_3^- to NO_2^- in this study resulted in a downregulation of the NR gene of *N. tangutorum*, which was consistent with the above-mentioned findings from previous studies. The present study found no change in the expression of four genes encoding NiR (1.7.1.4, 1.7.7.1, 1.7.1.15, and 1.7.2.2) during the catalytic conversion of NO_2^- to ammonia. However, some studies have shown that drought stress inhibits NO_3^- absorption, resulting in the downregulation of the NiR gene expression [71,72], implying that some genes encoding NiR in *N. tangutorum* may be unaffected by drought stress. One reason for this could be that *N. tangutorum* is a drought-tolerant plant.

The conversion of ammonia (NH_4^+) nitrogen to organic nitrogen compounds requires ammonia assimilation. GS and GOGAT should be combined in this process to produce glutamine and glutamic acid, which are the precursors to nitrogenous compounds [61,73]. As a result, the GS/GOGAT cycle is critical for nitrogen metabolism. Stress conditions have been shown to frequently inhibit the GS/GOGAT enzyme activity in plants [72,74]. For example, under drought stress, tea bud GS activity was significantly reduced [75], and *Brassica juncea* BjGS gene expression was downregulated under salt stress [76]. The present study found that the GS gene expression is up- and downregulated during ammonia assimilation, implying that drought stress inhibits the formation of glutamine in *N. tangutorum* leaves.

In plants, GOGAT is found in two forms: Fd-GOGAT and NADH-GOGAT [77–79]. In the present study, both forms were expressed. In the glutamate synthase pathway, which catalyzes the formation of glutamate, the expression of the NADH-GOGAT gene was downregulated; the expression of the Fd-GOGAT gene, which assists other genes in catalyzing glutamate formation, was upregulated, consistent with the results of previous studies in *Lotus corniculatus* [80], *Sporobolus stapfianus* [81], *Triticum aestivum* [82] and other species. In addition, during formamide synthesis from ammonia, the expression of the formamide enzyme gene was downregulated, carbon dioxide was converted into bicarbonate, and the expression of the carbonic anhydrase gene was upregulated or downregulated. Hence, in the nitrogen metabolism pathway, we thought that all the genes that can be differentially expressed may be sensitive to drought stress and cooperate with each other to help *N. tangutorum* to cope with drought conditions.

Under water stress, the stomata of plant leaves close, and the content of the green pigment is significantly affected [83–85]. The syntheses of ALA, protoporphyrin IX, and chlorophyll acid ester are the three main regulatory steps of chlorophyll anabolism [86]. Furthermore, ALA synthesis is also a rate-limiting factor in chlorophyll anabolism, directly affecting the chlorophyll content [87,88]. In the ALA synthesis pathway, we found that the expression of the glutamyl-tRNA synthase gene was downregulated under drought stress, but the expression of the glutamyl-tRNA reductase gene was upregulated. Furthermore, under drought stress, ALA could enhance the drought resistance of wheat chloroplasts by regulating the photosynthesis and ribosome metabolic pathways [89]. We also found that the expression of the glutamine-1-hemialdehyde transaminase gene was mainly downregulated, indicating that glutamyl-tRNA synthase can regulate downstream chlorophyll synthesis by regulating gene expression and ensure that *N. tangutorum* can cope with drought stress.

Another significant pathway is the synthesis of protoporphyrin IX; ALA is formed through a series of six reactions catalyzed by various enzymes [90]. To begin, ALA is condensed to form biliverdin, which is then deaminated by biliverdin deaminase to form hydroxymethyl biliary tryptophan. Hydroxymethyl biliary tryptophan is converted to pro-uroporphyrin I by biliverdin deaminase, and uroporphyrin III is synthesized by uroporphyrin III synthase. The carboxyl group of uroporphyrin III is removed and transformed into coproporphyrinogen III by uroporphyrin III decarboxylase. Coproporphyrinogen III is oxidized by coproporphyrinogen III oxidase and converted to protoporphyrin IX by protoporphyrinogen IX oxidase. The present study discovered that the biliverdin synthase gene expression was upregulated, indicating that drought stress initiated the function of δ -aminolevulinic acid dehydratase and regulated the ALA synthesized in the previous step to affect the biliverdin content under drought stress. This phenomenon was consistent with previous findings that plants may produce increased amounts of biliverdin in response to severe drought stress [91]. Following that, the uroporphyrin III synthase gene expression was upregulated to increase the uroporphyrin III content. Finally, the protoporphyrin peroxidase gene expression was upregulated to promote protoporphyrin IX synthesis, while another protoporphyrin peroxidase gene expression was upregulated to enhance coproporphyrin III synthesis. Changes in the expression of these enzymes worked in concert to overcome drought stress in *N. tangutorum*. However, it differs from the creeping bentgrass study's findings [92], which may be cultivar-specific.

Additionally, protoporphyrin IX acts as a common precursor in both directions during the final step of chlorophyll and heme syntheses [93]. The ferrous chelatase gene expression was up- and downregulated in the direction of heme synthesis, but the upregulated expression was greater than the downregulated expression. The expression of ferrous heme synthase and *COX15* was upregulated, resulting in increased ferrous heme synthesis. The feedback inhibition of heme is a regulatory step in chlorophyll synthesis, and both reducing the rate of heme degradation and inhibiting biliverdin formation mutations can reduce the formation of chlorophyllide, which is thought to be caused by heme restriction in ALA synthesis [94]. In other words, the heme may play a role in the transcriptional regulation of porphyrin biosynthesis genes in plants, allowing them to withstand drought-induced water stress [95]. Our research discovered that, when numerous genes were regulated, heme synthesis increased, and ALA synthesis decreased. The specific regulatory mechanism, on the other hand, must be identified. Magnesium chelatase is the second critical enzyme in chlorophyll synthesis, and its gene expression has a direct effect on chlorophyll synthesis [93,96]. Drought stress frequently results in a significant decrease in the chlorophyll *a*, chlorophyll *b*, and the total chlorophyll content of plants, as previously demonstrated [91,97,98]. The results of this study indicated that, under drought stress, the magnesium chelatase H subunit gene expression was downregulated more than it was upregulated, which might have had an effect on chlorophyll *a* synthesis. The expression of the downstream original chlorophyllin reductase was upregulated to promote the synthesis of original chlorophyllin *a*, but the expression of diethylene reductase was downregulated to inhibit the synthesis of chlorophyllin *a*, and the expression of the chlorophyll synthase gene was downregulated to affect the synthesis of chlorophyll *a* and chlorophyll *b*.

In the chlorophyll metabolic pathway, plants regulate themselves to prevent photosynthetic damage and degrade the excess chlorophyll into components without inducing photosynthetic toxicity. Studies have shown that converting chlorophyll *b* into chlorophyll *a* under the action of chlorophyll *b* reductase is one of the degradation pathways of chlorophyll [99]. According to this study, the expression of chlorophyll *b* reductase and 7-hydroxychlorophyll *a* reductase was found to be upregulated to improve the transformation ability of chlorophyll *b* into chlorophyll *a* and to accelerate chlorophyll degradation.

5. Conclusions

We identified 10,229 DEGs from *N. tangutorum* under drought stress. There were 3047 DEGs annotated to 119 classified metabolic pathways in the KEGG database, which

were mainly involved in the functions of ribosomes, plant hormone signal transduction, endoplasmic reticulum protein processing, porphyrin and chlorophyll metabolism, anthocyanin biosynthesis, and flavonoid biosynthesis. Nitrate reductase can resist drought stress by decreasing its activity, and drought stress can inhibit the formation of glutamine. In the pathway that catalyzes the formation of glutamate, GOGAT can assist other genes in catalyzing the formation of glutamate. Drought stress was found to decrease the synthesis of ALA and chlorophyll *a* and *b*, but increase the transformation ability of chlorophyll *b* into chlorophyll *a*. The present study provides novel, detailed genetic information and lays the foundation for better understanding the mechanisms that regulate the growth of sand xerophytes. This conceptual framework can guide future developments and the cultivation of new, drought-resistant genotypes. In addition, our findings provide a solid theoretical foundation for the long-term improvement of desert ecosystems.

Supplementary Materials: The following supporting information can be downloaded at <https://www.mdpi.com/article/10.3390/f13040509/s1>: Table S1. RNA sequencing statistics; Table S2. Lengths of transcripts and unigenes.

Author Contributions: C.L. and N.D. contributed equally to this paper. Conceptualization, C.L. and N.D.; methodology, C.L.; software, N.D.; validation, H.L., X.Z. and P.D.; formal analysis, C.L. and N.D.; investigation, C.L., N.D. and X.C.; resources, Q.L.; data curation, N.D. and X.C.; writing—original draft preparation, C.L.; writing—review and editing, N.D., J.W. and Q.L.; visualization, C.L. and N.D.; supervision, Q.L.; project administration, Q.L.; funding acquisition, N.D. and Q.L. All authors have read and agreed to the published version of the manuscript.

Funding: This research was supported by the National Natural Science Foundation of China (Grant No. 31470622), the National Key R&D Program of China during the 13th Five-year Plan Period (Grant No. 2019YFF030320102), and the National Forest Germplasm Resource Platform Construction and Operation Services (Grant No. 2005DKA21003).

Data Availability Statement: The data presented in this study are available on request from the corresponding author. The data are not publicly available due to ethical reasons.

Conflicts of Interest: The authors declare that they have no conflict of interest.

References

1. Cheng, H.F.; Hu, Y.A.; Zhao, J.F. Meeting China's water shortage crisis: Current practices and challenges. *Environ. Sci. Technol.* **2009**, *43*, 240–244. [[CrossRef](#)] [[PubMed](#)]
2. Zhang, L.; Chen, F.; Lei, Y.D. Climate change and shifts in cropping systems together exacerbate China's water scarcity. *Environ. Res. Lett.* **2020**, *15*, 104060. [[CrossRef](#)]
3. Huang, J.P.; Yu, H.P.; Guan, X.D.; Wang, G.Y.; Guo, R.X. Accelerated dryland expansion under climate change. *Nat. Clim. Chang.* **2016**, *6*, 166–171. [[CrossRef](#)]
4. Guo, Y.; Shen, Y. Agricultural water supply/demand changes under projected future climate change in the arid region of northwestern China. *J. Hydrol.* **2016**, *540*, 257–273. [[CrossRef](#)]
5. Li, X.Z.; Liu, X.D.; Ma, Z.G. Analysis on the drought characteristics in the main arid regions in the world since recent hundred-odd years. *Arid Zone Res.* **2004**, *21*, 97–103. (In Chinese)
6. Ebeed, H.T.; El-Helely, A.A. Programmed cell death in plants: Insights into developmental and stress-induced cell death. *Curr. Protein Pept. Sci.* **2021**, *22*, 873–889. [[CrossRef](#)]
7. Lai, L.M.; Chen, L.J.; Zheng, M.Q.; Jaing, L.H.; Zhou, J.H.; Zheng, Y.R.; Shimizu, H. Seed germination and seedling growth of five desert plants and their relevance to vegetation restoration. *Ecol. Evol.* **2019**, *9*, 2160–2170. [[CrossRef](#)]
8. Ebeed, H.T.; Hassan, N.M.; Keshta, M.M.; Hassanin, O.S. Comparative analysis of seed yield and biochemical attributes in different sunflower genotypes under different levels of irrigation and salinity. *Egypt. J. Bot.* **2019**, *59*, 339–355. [[CrossRef](#)]
9. Azad, N.; Rezayian, M.; Hassanpour, H.; Niknam, V.; Ebrahimzadeh, H. Physiological mechanism of salicylic acid in *Mentha pulegium* L. under salinity and drought stress. *Braz. J. Bot.* **2021**, *44*, 359–369. [[CrossRef](#)]
10. Hassan, N.; Ebeed, H.; Aljaarany, A. Exogenous application of spermine and putrescine mitigate adversities of drought stress in wheat by protecting membranes and chloroplast ultra-structure. *Physiol. Mol. Biol. Plants* **2020**, *26*, 233–245. [[CrossRef](#)]
11. Vanlerberghe, G.C.; Martyn, G.D.; Dahal, K. Alternative oxidase: A respiratory electron transport chain pathway essential for maintaining photosynthetic performance during drought stress. *Physiol. Plant.* **2016**, *157*, 322–337. [[CrossRef](#)] [[PubMed](#)]

12. Wang, W.; Wang, L.; Wang, L.; Tan, M.L.; Ogutu, C.O.; Yin, Z.Y.; Zhou, J.; Wang, J.M.; Wang, L.J.; Yan, X.C. Transcriptome analysis and molecular mechanism of linseed (*Linum usitatissimum* L.) drought tolerance under repeated drought using single-molecule long-read sequencing. *BMC Genom.* **2021**, *22*, 109. [[CrossRef](#)] [[PubMed](#)]
13. Sun, Y.J.; Zhou, J.; Guo, J. Advances in the knowledge of adaptive mechanisms mediating abiotic stress responses in *Camellia sinensis*. *Front. Biosci.-Landmark* **2021**, *26*, 1714–1722. [[CrossRef](#)] [[PubMed](#)]
14. Tezara, W.; Mitchell, V.; Driscoll, S.P.; Lawlor, D.W. Effects of water deficit and its interaction with CO₂ supply on the biochemistry and physiology of photosynthesis in sunflower. *J. Exp. Bot.* **2002**, *53*, 1781–1791. [[CrossRef](#)]
15. Zhou, Y.B.; Chen, M.; Guo, J.K.; Wang, Y.X.; Min, D.H.; Jiang, Q.Y.; Ji, H.T.; Huang, C.Y.; Wei, W.; Xu, H.J.; et al. Overexpression of the soybean (*Glycine max*) DRE-binding transcription factor GmDREB1 enhanced drought stress tolerance of transgenic wheat in the field. *J. Exp. Bot.* **2019**, *71*, 1842–1857. [[CrossRef](#)]
16. Alam, H.; Khattak, J.Z.K.; Ksiksi, T.S.; Saleem, M.H.; Fahad, S.; SoHail, H.; Ali, Q.; Zamin, M.; El-Esawi, M.A.; Saud, S.; et al. Negative impact of long-term exposure of salinity and drought stress on native *Tetraena mandavillei* L. *Physiol. Plant.* **2021**, *172*, 1336–1351. [[CrossRef](#)]
17. Brito, C.; Dinis, L.T.; Moutinho-Pereira, J.; Correia, C.M. Drought stress effects and olive tree acclimation under a changing climate. *Plants* **2019**, *8*, 232. [[CrossRef](#)]
18. Gessler, A.; Cailleret, M.; Joseph, J.; Schönbeck, L.; Schaub, M.; Lehmann, M.; Treydte, K.; Rigling, A.; Timofeeva, G.; Saurer, M. Drought induced tree mortality—a tree-ring isotope based conceptual model to assess mechanisms and predispositions. *New Phytol.* **2018**, *219*, 485490. [[CrossRef](#)]
19. DeSoto, L.; Cailleret, M.; Sterck, F.; Jansen, S.; Kramer, K.; Robert, E.M.R.; Aakala, T.; Amoroso, M.M.; Bigler, C.; Camarero, J.J.; et al. Low growth resilience to drought is related to future mortality risk in trees. *Nat. Commun.* **2020**, *11*, 1–9. [[CrossRef](#)]
20. Shao, Y.Y.; Zhang, Y.Q.; Wu, X.Q.; Bourque, C.P.A.; Zhang, J.T.; Qin, S.G.; Wu, B. Relating historical vegetation cover to aridity patterns in the greater desert region of northern China: Implications to planned and existing restoration projects. *Ecol. Indic.* **2018**, *89*, 528–537. [[CrossRef](#)]
21. Li, Q.H.; Jiang, Z.P. *Research on Nitraria tangutorum*; China Forestry Press: Beijing, China, 2011; p. 172. (In Chinese)
22. Li, S.H.; Mason, J.A.; Xu, Y.H.; Xu, C.; Zheng, G.; Li, J.C.; Yizhaq, H.; Pan, S.; Lu, H.Y.; Xu, Z.W. Biogeomorphology of nebkhas in the Mu Us dune field, north-central China: Chronological and morphological results. *Geomorphology* **2021**, *394*, 107979. [[CrossRef](#)]
23. Wei, Y.J.; Dang, X.H.; Wang, J.; Gao, J.L.; Gao, Y. Response of C:N:P in the plant-soil system and stoichiometric homeostasis of *Nitraria tangutorum* leaves in the oasis-desert ecotone, Northwest China. *J. Arid Land* **2021**, *13*, 934–946. [[CrossRef](#)]
24. Zhu, L.M.; Lu, L.; Yang, L.M.; Hao, Z.D.; Chen, J.H.; Cheng, T.L. The full-length transcriptome sequencing and identification of Na⁺/H⁺ antiporter genes in halophyte *Nitraria tangutorum* Bobrov. *Genes* **2021**, *12*, 836. [[CrossRef](#)] [[PubMed](#)]
25. Chen, T.T.; Zhou, Y.W.; Zhang, J.B.; Peng, Y.; Yang, X.Y.; Hao, Z.D.; Lu, Y.; Wu, W.H.; Cheng, T.L.; Shi, J.S.; et al. Integrative analysis of transcriptome and proteome revealed nectary and nectar traits in the plant-pollinator interaction of *Nitraria tangutorum* Bobrov. *BMC Plant Biol.* **2021**, *21*, 1–13. [[CrossRef](#)] [[PubMed](#)]
26. Lu, L.; Chen, X.Y.; Zhu, L.M.; Li, M.J.; Zhang, J.B.; Yang, X.Y.; Wang, P.K.; Lu, Y.; Cheng, T.L.; Shi, J.S.; et al. *NtCIPK9*: A calcineurin B-Like protein-interacting protein kinase from the halophyte *Nitraria tangutorum*, enhances *Arabidopsis* salt tolerance. *Front. Plant Sci.* **2020**, *11*, 1112. [[CrossRef](#)] [[PubMed](#)]
27. Gao, Z.Q.; Gao, S.; Li, X.P.; Zhnng, Y.; Ma, B.J.; Wang, Y.C. Exogenous methyl jasmonate promotes salt stress-induced growth inhibition and prioritizes defense response of *Nitraria tangutorum* Bobr. *Physiol. Plant.* **2021**, *172*, 162–175. [[CrossRef](#)]
28. Zhao, J.Q.; Wang, Y.M.; Yang, Y.L.; Zeng, Y.; Wang, Q.L.; Shao, Y.; Mei, L.J.; Shi, Y.P.; Tao, Y.D. Isolation and identification of antioxidant and α -glucosidase inhibitory compounds from fruit juice of *Nitraria tangutorum*. *Food Chem.* **2017**, *227*, 93–101. [[CrossRef](#)]
29. Abila, M.; Zha, X.; Wang, Y.; Wang, X.Y.; Gao, F.; Zhou, Y.J.; Feng, J.C. Characterization of the complete chloroplast genome of *Nitraria tangutorum*, a desert shrub. *J. Genet.* **2019**, *98*, 91. [[CrossRef](#)]
30. Zhan, J.P.; Li, G.S.; Ryu, C.H.; Ma, C.; Zhang, S.S.; Lloyd, A.; Hunter, B.G.; Larkins, B.A. Opaque-2 regulates a complex gene network associated with cell differentiation and storage functions of maize endosperm. *Plant Cell* **2018**, *30*, 2425–2446. [[CrossRef](#)]
31. Jia, S.J.; Li, H.W.; Jiang, Y.P.; Tang, Y.L.; Zhao, G.Q.; Zhang, Y.L.; Yang, S.J.; Qiu, H.S.; Wang, Y.C.; Guo, J.M.; et al. Transcriptomic analysis of female panicles reveals gene expression responses to drought stress in maize (*Zea mays* L.). *Agronomy* **2020**, *10*, 313. [[CrossRef](#)]
32. Gupta, A.; Rico-Medina, A.; Caño-Delgado, A.I. The physiology of plant responses to drought. *Science* **2020**, *368*, 266–269. [[CrossRef](#)] [[PubMed](#)]
33. Nguyen, T.L.; Bui, B.C. Fine mapping for drought tolerance in rice (*Oryza sativa* L.). *Omonrice* **2008**, *16*, 9–15.
34. Fàbregas, N.; Lozano-Elena, F.; Blasco-Escámez, D.; Tohge, T.; Martínez-Andújar, C.; Albacete, A.; Osorio, S.; Bustamante, M.; Riechmann, J.L.; Nomura, T.; et al. Overexpression of the vascular brassinosteroid receptor BRL3 confers drought resistance without penalizing plant growth. *Nat. Commun.* **2018**, *9*, 4680. [[CrossRef](#)]
35. Deyholos, M.K. Making the most of drought and salinity transcriptomics. *Plant Cell Environ.* **2010**, *33*, 648–654. [[CrossRef](#)] [[PubMed](#)]
36. Costa, V.; Angelini, C.; Feis, I.; Ciccodicola, A. Uncovering the complexity of transcriptomes with RNA-seq. *J. Biomed. Biotechnol.* **2010**, *2010*, 1–19. [[CrossRef](#)] [[PubMed](#)]

37. Kumar, V.; Hainaut, M.; Delhomme, N.; Mannapperuma, C.; Immerzeel, P.; Street, N.R.; Henrissat, B.; Mellerowicz, W.J. Poplar carbohydrate-active enzymes: Whole-genome annotation and functional analyses based on RNA expression data. *Plant J.* **2019**, *99*, 589–609. [[CrossRef](#)]
38. Yang, J.L.; Wang, H.Z.; Zhao, S.C.; Liu, X.; Zhang, X.; Wu, W.L.; Li, C.H. Overexpression levels of *LbDREB6* differentially affect growth, drought, and disease tolerance in poplar. *Front. Plant Sci.* **2020**, *11*, 1661. [[CrossRef](#)]
39. Wei, W.; Liang, D.W.; Bian, X.H.; Shen, M.; Xiao, J.H.; Zhang, W.K.; Ma, B.; Lin, Q.; Lv, J.; Chen, X.; et al. GmWRKY54 improves drought tolerance through activating genes in abscisic acid and Ca²⁺ signaling pathways in transgenic soybean. *Plant J.* **2019**, *100*, 384–398. [[CrossRef](#)]
40. Wang, K.; Bu, T.T.; Cheng, Q.; Dong, L.D.; Su, T.; Chen, Z.M.; Kong, F.J.; Gong, Z.Z.; Liu, B.H.; Li, M.N. Two homologous *LHY* pairs negatively control soybean drought tolerance by repressing the abscisic acid responses. *New Phytol.* **2020**, *229*, 2660–2675. [[CrossRef](#)]
41. Danilevskaia, O.N.; Yu, G.X.; Meng, X.; Xu, J.; Stephenson, E.; Estrada, S.; Chilakamarri, S.; Zastrow-Hayes, G.; Thatcher, S. Developmental and transcriptional responses of maize to drought stress under field conditions. *Plant Direct* **2019**, *3*, e00129. [[CrossRef](#)]
42. Wang, M.M.; Qu, H.B.; Zhang, H.D.; Liu, S.; Li, Y.; Zhang, C.Q. Hormone and RNA-seq analyses reveal the mechanisms underlying differences in seed vigour at different maize ear positions. *Plant Mol. Biol.* **2019**, *99*, 461–476. [[CrossRef](#)] [[PubMed](#)]
43. Li, Q.H.; Xin, Z.M.; Gao, T.T.; Wang, S.X.; Xu, J.; Sun, F. Reproductive allocation in four desert species of the genus *Nitraria* L. *Acta Ecol. Sin.* **2012**, *32*, 5054–5061. (In Chinese)
44. Kang, J.J.; Zhao, W.Z.; Zhao, M.; Zheng, Y.; Yang, F. NaCl and Na₂SiO₃ coexistence strengthens growth of the succulent xerophyte *Nitraria tangutorum* under drought. *Plant Growth Regul.* **2015**, *77*, 223–232. [[CrossRef](#)]
45. Ren, Y.; Lu, Q.; Wu, B.; Liu, M.H. Specific leaf area and leaf dry matter content of *Nitraria tangutorum* in the artificially simulated precipitation. *Acta Ecol. Sin.* **2015**, *35*, 4707–4715. (In Chinese)
46. Kang, J.J.; Zhao, W.Z.; Zhou, H.; Wang, Z.W. The features of main osmolytes, silicon and their coupling effects in improving drought resistance of the typical xerophytes in the desert areas of Northwest China. *Land Degrad. Dev.* **2020**, *31*, 2720–2733. [[CrossRef](#)]
47. Anders, S.; Huber, W. Differential expression analysis for sequence count data. *Genome Biol.* **2010**, *11*, R106. [[CrossRef](#)] [[PubMed](#)]
48. Tao, G.Y.; Ramakrishnan, M.; Vinod, K.K.; Yrjälä, K.; Satheesh, V.; Cho, J.; Fu, Y.; Zhou, M.B. Multi-omics analysis of cellular pathways involved in different rapid growth stages of moso bamboo. *Tree Physiol.* **2020**, *40*, 1487–1508. [[CrossRef](#)]
49. Novaes, E.; Drost, D.R.; Farmerie, W.G.; Pappas, G.J., Jr.; Grattapaglia, D.; Sederoff, R.; Kirst, M. High-throughput gene and SNP discovery in *Eucalyptus grandis*, an uncharacterized genome. *BMC Genom.* **2008**, *9*, 312. [[CrossRef](#)]
50. Zhou, X.H.; Bao, S.Y.; Liu, J.; Zhuang, Y. De novo sequencing and analysis of the transcriptome of the wild eggplant species *Solanum aculeatissimum* in response to *Verticillium dahliae*. *Plant Mol. Biol. Rep.* **2016**, *34*, 1193–1203. [[CrossRef](#)]
51. Hou, R.; Bao, Z.M.; Wang, S.; Su, H.L.; Li, Y.; Du, H.X.; Hu, J.J.; Wang, S.; Hu, X.L. Transcriptome sequencing and *De Novo* analysis for yesso scallop (*Patinopecten yessoensis*) Using 454 GS FLX. *PLoS ONE* **2011**, *6*, e21560. [[CrossRef](#)]
52. Long, Y.; Zhang, J.; Tian, X.; Wu, S.; Zhang, Q.; Zhang, J.; Zhang, D.; Pei, X. De novo assembly of the desert tree *Haloxylon ammodendron* (C. A. Mey.) based on RNA-seq data provides insight into drought response, gene discovery and marker identification. *BMC Genom.* **2014**, *15*, 1111. [[CrossRef](#)] [[PubMed](#)]
53. Wu, Y.; Wei, W.; Pang, X.; Wang, X.; Zhang, H.; Dong, B.; Xing, Y.; Li, X.; Wang, M. Comparative transcriptome profiling of a desert evergreen shrub, *Ammopiptanthus mongolicus*, in response to drought and cold stresses. *BMC Genom.* **2014**, *15*, 671. [[CrossRef](#)] [[PubMed](#)]
54. Kim, S.; Na, J.; Nie, H.; Kim, J.; Lee, J.; Kim, S. Comprehensive transcriptome profiling of *Caragana microphylla* in response to salt condition using de novo assembly. *Biotechnol. Lett.* **2021**, *43*, 317–327. [[CrossRef](#)] [[PubMed](#)]
55. Ye, G.S.; Ma, Y.H.; Feng, Z.P.; Zhang, X.F. Transcriptomic analysis of drought stress responses of sea buckthorn (*Hippophae rhamnoides* subsp. *sinensis*) by RNA-Seq. *PLoS ONE* **2018**, *13*, e0202213. [[CrossRef](#)]
56. Mahmood, T.; Khalid, S.; Abdullah, M.; Ahmed, Z.; Shah, M.K.N.; Ghafoor, A.; Du, X.M. Insights into drought stress signaling in plants and the molecular genetic basis of cotton drought tolerance. *Cells* **2019**, *9*, 105. [[CrossRef](#)]
57. Chen, X.X.; Ding, Y.L.; Yang, Y.Q.; Song, C.P.; Wang, B.S.; Yang, S.H.; Guo, Y.; Gong, Z.Z. Protein kinases in plant responses to drought, salt, and cold stress. *J. Integr. Plant Biol.* **2021**, *63*, 53–78. [[CrossRef](#)]
58. Chen, Q.C.; Hu, T.; Li, X.H.; Song, Y.W.; Zhu, J.K.; Chen, L.Q.; Zhao, Y. Phosphorylation of SWEET sucrose transporters regulates plant root: Shoot ratio under drought. *Nat. Plants* **2022**, *8*, 68–77. [[CrossRef](#)]
59. Li, W.; Fu, L.F.; Geng, Z.W.; Zhao, X.J.; Liu, Q.H.; Jiang, X.Q. Physiological characteristic changes and full-length transcriptome of rose (*Rosa chinensis*) roots and leaves in response to drought stress. *Plant Cell Physiol.* **2020**, *61*, 2153–2166. [[CrossRef](#)]
60. Wang, Y.Y.; Hsu, P.K.; Tsay, Y.F. Uptake, allocation and signaling of nitrate. *Trends Plant Sci.* **2012**, *17*, 458–467. [[CrossRef](#)]
61. Zhang, C.X.; Meng, S.; Li, M.J.; Zhao, Z. Transcriptomic insight into nitrogen uptake and metabolism of *Populus simonii* in response to drought and low nitrogen stresses. *Tree Physiol.* **2018**, *38*, 1672–1684. [[CrossRef](#)]
62. Cai, H.M.; Xiao, J.H.; Zhang, Q.F.; Lian, X.M. Co-suppressed *glutamine synthase 2* gene modifies nitrogen metabolism and plant growth in rice. *Chin. Sci. Bull.* **2010**, *55*, 871–882. [[CrossRef](#)]
63. Xu, X.; Fu, X.; Liao, H. Advances in study of ammonium assimilation and its regulatory mechanism in plants. *Bull. Bot.* **2016**, *51*, 152–166. (In Chinese)

64. Campbell, W.H. Nitrate reductase and its role in nitrate assimilation in plants. *Physiol. Plant.* **1988**, *74*, 214–219. [[CrossRef](#)]
65. Caravaca, F.; Figueroa, D.; Barea, J.M.; Azcón-Aguilar, C.; Roldán, A. Effect of mycorrhizal inoculation on nutrient acquisition, gas exchange, and nitrate reductase activity of two Mediterranean-autochthonous shrub species under drought stress. *J. Plant Nutr.* **2004**, *27*, 57–74. [[CrossRef](#)]
66. Chamizo-Ampudia, A.; Sanz-Luque, E.; Llamas, A.; Galvan, A.; Fernandez, E. Nitrate reductase regulates plant nitric oxide homeostasis. *Trends Plant Sci.* **2017**, *22*, 163–174. [[CrossRef](#)]
67. Han, R.C.; LI, C.Y.; Rasheed, A.; Pan, X.H.; Shi, Q.H.; Wu, Z.M. Reducing phosphorylation of nitrate reductase improves nitrate assimilation in rice. *J. Integr. Agric.* **2022**, *21*, 15–25. [[CrossRef](#)]
68. Han, M.L.; Lv, Q.Y.; Zhang, J.; Wang, T.; Zhang, C.X.; Tan, R.J.; Wang, T.L.; Zhong, L.Y.; Gao, Y.Q.; Chao, Z.F.; et al. Decreasing nitrogen assimilation under drought stress by suppressing DST-mediated activation of nitrate reductase 1.2 in rice. *Mol. Plant* **2021**, *15*, 167–178. [[CrossRef](#)]
69. Yadav, R.S.; Sharwa, R.L.; Pandey, U.K. Effects of various water potential treatment on nitrogen reductase activity in wheat genotypes. *Agric. Sci. Digest.* **1998**, *18*, 73–75.
70. Robredo, A.; Perez-Lopez, U.; Miranda-Apodaca, J.; Lacuesta, M.; Mena-Petite, A.; Munoz-Rueda, A. Elevated CO₂ reduces the drought effect on nitrogen metabolism in barley plants during drought and subsequent recovery. *J. Exp. Bot.* **2011**, *71*, 399–408. [[CrossRef](#)]
71. Sanchez-Rodriguez, E.; Rubio-Wilhelmi, M.d.M.; Rios, J.J.; Blasco, B.; Rosales, M.A.; Melgarejo, R.; Romero, L.; Ruiz, J.M. Ammonia production and assimilation: Its importance as a tolerance mechanism during moderate water deficit in tomato plants. *J. Plant Physiol.* **2011**, *168*, 816–823. [[CrossRef](#)]
72. Meng, S.; Zhang, C.X.; Su, L.; Li, Y.M.; Zhao, Z. Nitrogen uptake and metabolism of *Populus simonii* in response to PEG-induced drought stress. *Environ. Exp. Bot.* **2016**, *123*, 78–87. [[CrossRef](#)]
73. Liu, Y.L.; Duan, X.L.; Zhao, X.D.; Ding, W.L.; Wang, Y.W.; Xiong, Y. Diverse nitrogen signals activate convergent ROP2-TOR signaling in Arabidopsis. *Dev. Cell* **2021**, *56*, 1283–1295.e5. [[CrossRef](#)] [[PubMed](#)]
74. Rubio-Wilhelmi, M.d.M.; Sanchez-Rodriguez, E.; Leyva, R.; Blasco, B.; Romero, L.; Blumwald, E.; Ruiz, J.M. Response of carbon and nitrogen-rich metabolites to nitrogen deficiency in PSARK:: IPT tobacco plants. *Plant Physiol. Biochem.* **2012**, *57*, 231–237. [[CrossRef](#)] [[PubMed](#)]
75. Rana, N.K.; Mohanpuria, P.; Yadav, S.K. Expression of tea cytosolic glutamine synthetase is tissue specific and induced by cadmium and salt stress. *Biol. Plant.* **2008**, *52*, 361–364. [[CrossRef](#)]
76. Goel, P.; Singh, A.K. Abiotic stresses downregulate key genes involved in nitrogen uptake and assimilation in *Brassica juncea* L. *PLoS ONE* **2015**, *10*, e0143645.
77. Bowsher, C.G.; Lacey, A.E.; Hanke, G.T.; Clarkson, D.T.; Saker, L.R.; Stulen, L.; Emes, M.J. The effect of Glc6P uptake and its subsequent oxidation within pea root plastids on nitrite reduction and glutamate synthesis. *J. Exp. Bot.* **2007**, *58*, 1109–1118. [[CrossRef](#)]
78. Wang, Q.; Nian, J.Q.; Xie, X.Z.; Yu, H.; Zhang, J.; Bai, J.T.; Dong, G.J.; Hu, J.; Bo, B.; Chen, L.C.; et al. Genetic variations in ARE1 mediate grain yield by modulating nitrogen utilization in rice. *Nat. Commun.* **2018**, *9*, 1–10. [[CrossRef](#)]
79. Yoneyama, T.; Suzuki, A. Exploration of nitrate-to-glutamate assimilation in non-photosynthetic roots of higher plants by studies of 15N-tracing, enzymes involved, reductant supply, and nitrate signaling: A review and synthesis. *Plant Physiol. Biochem.* **2019**, *136*, 245–254. [[CrossRef](#)]
80. Borsani, O.; Diaz, P.; Monza, J. Proline is involved in water stress responses of *Lotus corniculatus* nitrogen fixing and nitrate fed plants. *J. Plant Physiol.* **1999**, *155*, 269–273. [[CrossRef](#)]
81. Martinelli, T.; Whittaker, A.; Boichichio, A.; Vazzana, C.; Suzuki, A.; Masclaux-Daubresse, C. Amino acid pattern and glutamate metabolism during dehydration stress in the ‘resurrection’ plant *Sporobolus stapfianus*: A comparison between desiccation-sensitive and desiccation-tolerant leaves. *J. Exp. Bot.* **2007**, *58*, 3037–3046. [[CrossRef](#)]
82. Curtis, T.Y.; Bo, V.; Tucker, A.; Halford, N. Construction of a network describing asparagine metabolism in plants and its application to the identification of genes affecting asparagine metabolism in wheat under drought and nutritional stress. *Food Energy Secur.* **2018**, *7*, e00126. [[CrossRef](#)] [[PubMed](#)]
83. Bota, J.; Medrano, H.; Flexas, J. Is photosynthesis limited by decreased RuBisCo activity and RuBP content under progressive water stress? *New Phytol.* **2010**, *162*, 671–681. [[CrossRef](#)] [[PubMed](#)]
84. Lang, Y.; Wang, M.; Xia, J.B.; Zhao, Q.K. Effects of soil drought stress on photosynthetic gas exchange traits and chlorophyll fluorescence in *Forsythia suspensa*. *J. For. Res.* **2018**, *29*, 45–53. [[CrossRef](#)]
85. Zhuang, J.; Wang, Y.L.; Chi, Y.G.; Zhou, L.; Chen, J.J.; Zhou, W.; Song, J.; Zhao, N.; Ding, J.X. Drought stress strengthens the link between chlorophyll fluorescence parameters and photosynthetic traits. *PeerJ* **2020**, *8*, e10046. [[CrossRef](#)] [[PubMed](#)]
86. Cornah, J.E.; Terry, M.J.; Smith, A.G. Green or red: What stops the traffic in the tetrapyrrole pathway. *Trends Plant Sci.* **2003**, *8*, 224–230. [[CrossRef](#)]
87. Richter, A.; Peter, E.; Pors, Y.; Lorenzen, S.; Grimm, B.; Czarnecki, O. Rapid dark repression of 5-aminolevulinic acid synthesis in green barley leaves. *Plant Cell Physiol.* **2010**, *51*, 670–681. [[CrossRef](#)]
88. Santos, C.V. Regulation of chlorophyll biosynthesis and degradation by silt stress in sunflower leaves. *Sci. Hortic.* **2004**, *103*, 93–99. [[CrossRef](#)]

89. Wang, Y.X.; Li, X.Y.; Liu, N.N.; Wei, S.M.; Wang, J.N.; Qin, F.J.; Suo, B. The iTRAQ-based chloroplast proteomic analysis of *Triticum aestivum* L. leaves subjected to drought stress and 5-aminolevulinic acid alleviation reveals several proteins involved in the protection of photosynthesis. *BMC Plant Biol.* **2020**, *20*, 1–17. [[CrossRef](#)]
90. Beale, S. Green genes gleaned. *Trends Plant Sci.* **2005**, *10*, 309–312. [[CrossRef](#)]
91. Ma, Q.L.; Xu, X.; Xie, Y.Z.; Huang, T.; Wang, W.J.; Zhao, L.J. Comparative metabolomic analysis of the metabolism pathways under drought stress in alfalfa leaves. *Environ. Exp. Bot.* **2021**, *183*, 104329. [[CrossRef](#)]
92. Merewitz, E.; Xu, Y.; Huang, B. Differentially expressed genes associated with improved drought tolerance in creeping bentgrass overexpressing a gene for cytokinin biosynthesis. *PLoS ONE* **2016**, *11*, e0166676. [[CrossRef](#)] [[PubMed](#)]
93. Zhang, D.; Chang, E.J.; Yu, X.X.; Chen, Y.H.; Yang, Q.S.; Cao, Y.T.; Li, X.K.; Wang, Y.H.; Fu, A.G.; Xu, M. Molecular characterization of Magnesium Chelatase in soybean [*Glycine max* (L.) Merr.]. *Front Plant Sci.* **2018**, *9*, 720. [[CrossRef](#)] [[PubMed](#)]
94. Terry, M.J.; Kendrick, R.E. Feedback inhibition of chlorophyll synthesis in the phytochrome chromophore-deficient aurea and yellow-green 2 mutants of tomato. *Plant Physiol.* **1999**, *119*, 143–152. [[CrossRef](#)] [[PubMed](#)]
95. Phung, T.H.; Jung, H.; Park, J.H.; Kim, J.G.; Back, K.; Jung, S. Porphyrin biosynthesis control under water stress: Sustained porphyrin status correlates with drought tolerance in transgenic rice. *Plant Physiol.* **2011**, *157*, 1746–1764. [[CrossRef](#)] [[PubMed](#)]
96. Liu, L.L.; Lin, N.; Liu, X.Y.; Yang, S.; Wang, W.; Wan, X.C. From chloroplast biogenesis to chlorophyll accumulation: The interplay of light and hormones on gene expression in *Camellia sinensis* cv. *Shuchazao* Leaves. *Front. Plant Sci.* **2020**, *11*, 256. [[CrossRef](#)] [[PubMed](#)]
97. Jaleel, C.A.; Gopi, R.; Sankar, B.; Gomathinayagam, M.; Panneerselvam, R. Differential responses in water use efficiency in two varieties of *Catharanthus roseus* under drought stress. *Comptes Rendus Biol.* **2008**, *331*, 42–47. [[CrossRef](#)] [[PubMed](#)]
98. Kaur, G.; Asthir, B. Molecular responses to drought stress in plants. *Biol. Plant.* **2017**, *61*, 201–209. [[CrossRef](#)]
99. Sato, Y.; Morita, R.; Nishimura, M.; Yamaguchi, H.; Kusaba, M. Mendel's green cotyledon gene encodes a positive regulator of the chlorophyll-degrading pathway. *Proc. Natl. Acad. Sci. USA* **2007**, *104*, 14169–14174. [[CrossRef](#)]